Front. Mech. Eng. 2021, 16(2): 410–419
https://doi.org/10.1007/s11465-020-0618-y

RESEARCH ARTICLE

Chao CHEN, Huiyang ZHANG, Shengdun ZHAO, Xiaoqiang REN

Effects of sheet thickness and material on the mechanical properties of flat clinched joint

Abstract The flat clinching process is attracting a growing attention in the joining field of lightweight materials because it avoids the geometric protrusion that appears in the conventional clinching process. In this paper, the effects of sheet thickness and material on the mechanical properties of the clinched joint were studied. Al1060 and Al2024 sheets with 2 mm thickness were employed to develop the clinched joint by using different material configurations, and Al1060 sheets with 2.5- and 1.5-mm thicknesses were used to produce the clinched joint by using different thickness configurations. The clinched joints using various sheet configurations were sectioned, and dimensional analysis was conducted. Cross-tensile and shearing tests were carried out to analyze the mechanical properties of the clinched joint, including tensile strength, shearing strength, and absorbed energy. In addition, the failure modes of the clinched joints were discussed. Results indicated that the clinched joint with a stiff top sheet had increased static strength regardless of the test type. The clinched joint with a thick top sheet demonstrated lower static strength than the joint with a thick bottom sheet in the cross-tensile test. However, this result was reversed in the shearing tests. The flat clinching process has a great potential in joining dissimilar and various thickness materials.

Keywords clinched joint, flat clinching process, thickness configuration, material configuration, mechanical property

Received July 19, 2020; accepted November 1, 2020

Chao CHEN (✉), Huiyang ZHANG, Xiaoqiang REN
State Key Laboratory of High-Performance Complex Manufacturing, Light Alloy Research Institute, Central South University, Changsha 410083, China; School of Mechanical and Electrical Engineering, Central South University, Changsha 410083, China
E-mail: profchenchao@163.com

Shengdun ZHAO
School of Mechanical Engineering, Xi'an Jiaotong University, Xi'an 710049, China

1 Introduction

Driven by environmental protection and energy conservation, lightweight materials, especially lightweight metal materials with pronounced strength capacity, are increasingly employed in the field of machinery manufacturing [1–3]. The connection of lightweight materials has become a hot research topic. Conventional welding techniques are somewhat weak because of metal materials with complex joining conditions, such as dissimilar, painted, and coated [4–6]. In recent years, mechanical clinching technology has received increasing attention in this regard. It has numerous advantages, such as low cost, no additional materials introduced, and high dynamic strength [7–10].

The conventional mechanical clinching process can join two or more sheets by using a customized punch (e.g., rectangular or round punches [11,12]) and a special die (e.g., a TOG-L-LOC type involving extensible dies and a TOX type using a fixed die [13,14]). The clinched joint produced by a rectangular punch cannot bear nominally equal loading in all directions with high maximum shearing loads [11]. A round punch is more widely employed in this process because the clinched joint produced by a round punch avoids this problem. This process using a round punch has been successfully used in the building component, domestic appliance, and automotive industries [15,16]. It can connect many materials used in car body production, including aluminum alloy [15], magnesium alloy [17], and high-strength steel [9,18]. However, the connection of high-strength materials leads to increased wear of the clinching tools during this process [19]. In addition, a geometric protrusion at the die-sided sheet restricts the applied range of this process, particularly in the aesthetic requirements and functional areas.

Die-less clinching, in which extensile dies or a fixed die is replaced by a planar anvil, is a novel process used to reduce the height of geometric protrusion and the clinching tools wear [17,20,21]. Flat clinching, one kind of die-less clinching process, can completely avoid the emergence of protrusion at the die-sided sheet. Given this advantage, flat clinching has attracted the attention of many researchers. Gerstmann and Awiszus [22] and Lambiase [12] compared the static strengths of the flat clinched joint and conventional clinched joint. The flat clinched joint had a larger shearing strength and a smaller tensile strength than the other one. Lüder et al. [23] found that moisture content has a fundamental effect on the flat clinched connection by using aluminum and wood materials. Han et al. [24] optimized the geometrical dimensions of the punch and clamp in the flat clinching process through numerical simulations and experiments. Chen et al. [25] analyzed the static strengths, material flow, and failure modes of the flat clinching joints developed using various maximum forming forces. The clamping force must be sufficient to ensure that the bottom sheet is fixed on the planar anvil [26].

Thickness configuration has a considerable effect on the joint strength for the conventional clinching process. Varis [11,27] employed square and round clinching tools to compare the mechanical behavior of the clinched high-strength sheet metals with different thicknesses. Mucha et al. [9] proposed that the thickness configuration directly affects the load-carrying ability of the final joint. In the conventional and the reshaping processes, the clinched joint utilizing a thin top sheet could achieve a weaker neck portion than the joint with a thick top sheet [28,29]. In addition, automobile bodies are constructed using many sheets with various thicknesses. Therefore, the influence of thickness configuration on the flat clinched joint should also be investigated.

Material configuration plays an essential role in the conventional clinching process. Hamel et al. [14] analyzed the effect of material configuration on the geometric parameters of the clinched joint through finite element method (FEA) and experiments. He et al. [30] used Al5052, H62, and TA1 to understand the effect of material configuration on the shearing strength of the clinched joint with TOG-L-LOC configuration. Chen et al. [31] compared two compressing methods of clinched joints by using Al5052 and Al6061 sheets. The Al6061 sheet was better used as the top sheet to gain larger static strength than the Al5052 sheet. Chu et al. [4] proposed that sheet material with higher hardness and strength is appropriate to be employed as the top sheet during the clinching process. Of course, material configuration influences the mechanical properties of the flat joining. However, because flat clinching is a novel type of sheet joining process, few papers have reported this aspect.

In this paper, Al2024 and Al1060 sheets were employed to study the influence of the material on the flat clinching process. The effect of sheet thickness on the mechanical properties of the flat clinched joint was also investigated using the Al1060 sheets with 1.5- and 2.5-mm thickness. The flat clinching process was carried out to develop clinched joints under a 90 kN forming force. Cross-tensile and shearing tests were implemented to understand the mechanical properties of the clinched joint, including the static strength and absorbed energy. The failure modes of the joints were also analyzed and discussed. The flat clinching process has a great potential in joining dissimilar materials and those with various thicknesses.

2 Background of the flat clinching process

Flat clinching is a metal joining process where two or more metal sheets are connected by local plastic deformation. A set of clinching tools illustrated in Fig. 1 are designed to control the material flow of the top and bottom sheets. Under the action of deep displacement of the punch, the sheets near punch are dramatically thinned. A mechanical interlock is generated to hook the top and bottom sheets. Given no extra material involved and the effect of temperature, the static mechanical properties of the clinched joint depend mainly on its geometrical profile [32–34], especially the neck thickness (N_t) and interlock depth (U_d) depicted in Fig. 1(c).

A significantly large clamping force is required to keep the bottom sheet and the planar anvil aligned at all times and avoid a geometrical protrusion from appearing in the bottom sheet. Correspondingly, the material of the top sheet flows into the gap between the clamp and the punch, and an annular protrusion arises at the top sheet. Although this process requires a larger forming force and consumes more energy than the conventional clinching process, it also has the following benefits: Lower wear and costs of the clinched tools, no need for coaxial alignment of lower and upper dies, and components can be heated up directly

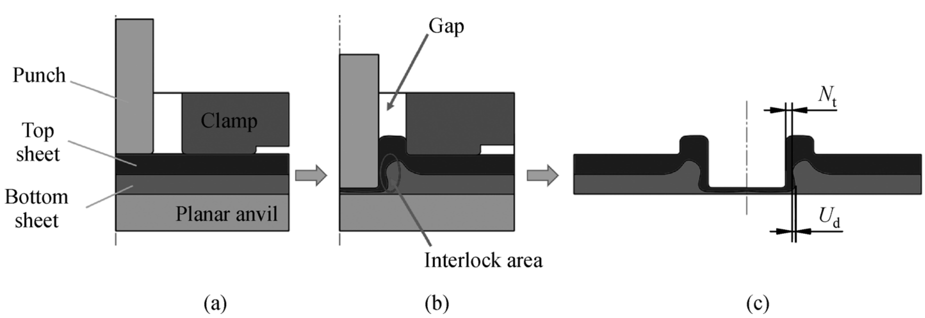

Fig. 1 Schematics of the flat clinching process: (a) The initial phase, (b) the interlocking phase, and (c) the resulting clinched joint.

on the planar anvil and then quickly joined. More importantly, it can be employed in aesthetic requirements and visible areas owing to a completely flat lower surface of the produced clinched joint.

The failure behavior of the joint is a manifestation of its mechanical properties. In the static tests, the flat clinched joint has three main failure modes [3,7,35–37], namely, unbuttoning, neck fracture, and hybrid failure, as illustrated in Fig. 2. The structural strengths of the neck portion (F_n) and that of the interlock (F_u) determine the failure modes of the clinched joints. The clinching joint loses efficiency in the unbuttoning mode when $F_n >> F_u$. The clinched joint fails in the neck fracture mode when $F_u >> F_n$. When $F_u \approx F_n$, that is, when the two structural strengths are similar, the clinched joint fails in the hybrid failure mode.

3 Materials and methods

3.1 Sheet material

The sheet specimens used in this study were made of aluminum alloys Al2024 and Al1060. The Al1060 sheets with nominal thicknesses of 2, 1.5, and 2.5 mm, and the Al2024 sheets with nominal thicknesses of 2.0 mm were cut along the rolling direction from three large Al1060 plates and a large Al2024 plate, respectively. The length of the sheet specimen was 80 mm, and its width was 25 mm. The main mechanical properties of both sheets are presented in Table 1. They had excellent ductility, which is a good condition for manufacturing high-quality flat clinched joints.

3.2 Flat clinching tests

Flat clinching tests were carried out using an Instron 5982 testing machine. Schematics of the flat clinching tools are depicted in Fig. 3. The flat clinching tools were designed to develop flat clinched samples. They were mainly composed of a planar anvil, a clamp, disc springs, and a punch. A forming load at a speed of 30 mm/min was preset to drive the punch to move vertically downward. When the forming load reached 90 kN, the forming load was released. In accordance with sheet configurations, the flat clinched samples were divided into the four types shown in Table 2. The 1060 + 2024 sample and 2024 + 1060 sample had different material configurations, while the

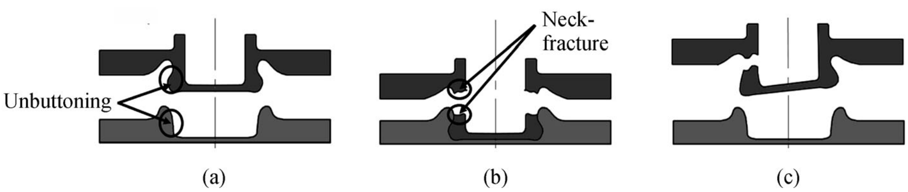

Fig. 2 Schematics of the failure modes occurring in the clinched joints: (a) Unbuttoning, (b) neck fracture, and (c) hybrid failure.

Table 1 Main mechanical properties of Al2024 and Al1060 sheets

Material	Young's modulus/GPa	Yield strength/MPa	Tensile strength/MPa	Poisson's ratio
Al2024	73.8	340.6	472.3	0.33
Al1060	68.5	95.3	120.5	0.33

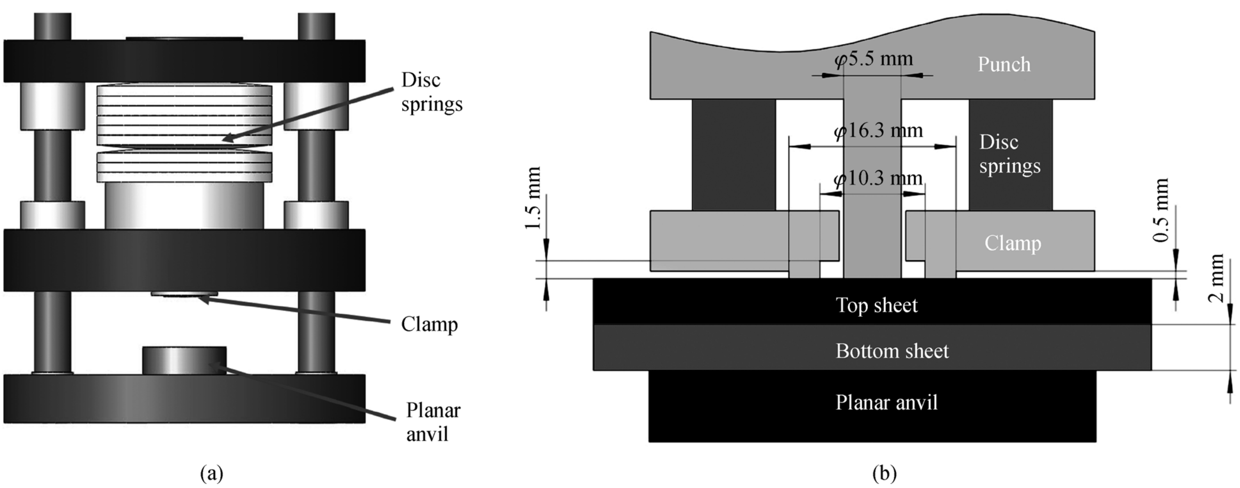

Fig. 3 Schematic of the flat clinching tools: (a) 3D model and (b) 2D model of the core flat clinching tools.

Table 2 Arrangement of the flat clinched samples

Flat clinched sample	Material of top sheet	Material of bottom sheet	Thickness of top sheet/mm	Thickness of bottom sheet/mm
1060 + 2024	Al1060	Al2024	2.0	2.0
2024 + 1060	Al2024	Al1060	2.0	2.0
1.5 + 2.5	Al1060	Al1060	1.5	2.5
2.5 + 1.5	Al1060	Al1060	2.5	1.5

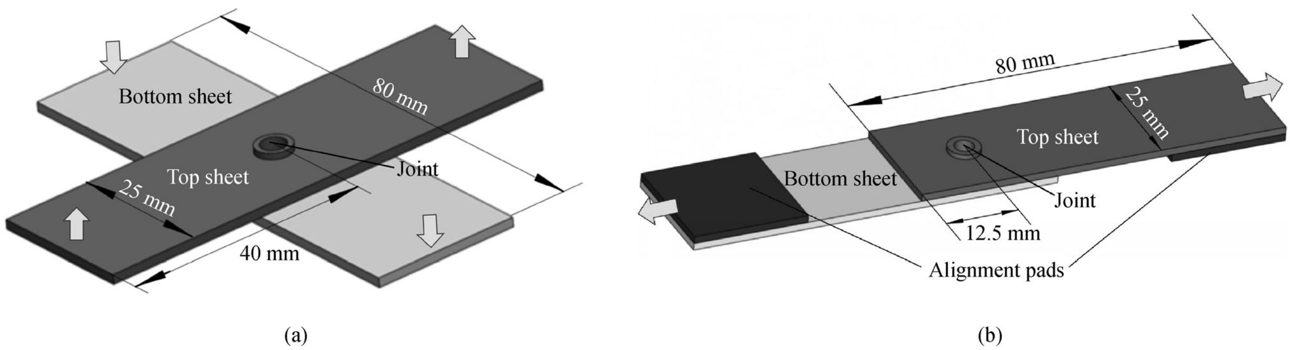

Fig. 4 Schematics of clinched samples in the clinched sample used in (a) the cross-tensile test and (b) the shearing test.

1.5 + 2.5 sample and 2.5 + 1.5 sample had different thickness configurations. For each type of sample, the flat clinching test was performed nine times.

3.3 Geometrical profiles and mechanical properties of clinched samples

Three clinched samples for each sheet configuration were sectioned along their respective centerlines by wire electrical discharge machining to observe the geometrical profile of the clinched joint. The cross-sectional profile of the clinched joint was observed using an optical microscope. The main characteristic parameters of the joint (N_t and U_d) were measured, and dimensional analysis was conducted.

Static strength is an important component of the mechanical properties of the clinched joint. Shearing and tensile strengths are two different static-strength types. In this study, they were obtained by conducting shearing and cross-tensile tests. The clinched samples employed in both tests were depicted in Fig. 4. Two alignment pads were used to concentrate the load for all configurations during the shearing tests. The load–displacement curves were measured and recorded by the Instron 5982 testing machine, and the maximum load (F_{max}) was employed as the static strength of the clinched joint. Three clinched samples were tested for each sheet configuration to calculate their average strength in the shearing and cross-tensile tests. The tests were implemented using the Instron 5982 testing machine with a full-scale load of 100 kN at a speed of 2 mm/min until the bottom and top sheets were completely separated.

As depicted in Fig. 5, the absorbed energy (E_n) [7,38,39], which belongs to the mechanical properties of the clinched joint, is an important assessment criterion of joining reliability. The area between the load curve and the displacement abscissa was measured to show the absorbed energy value of the clinched joint. The larger the energy absorbed by the clinched joint, the higher the reliability of the joining.

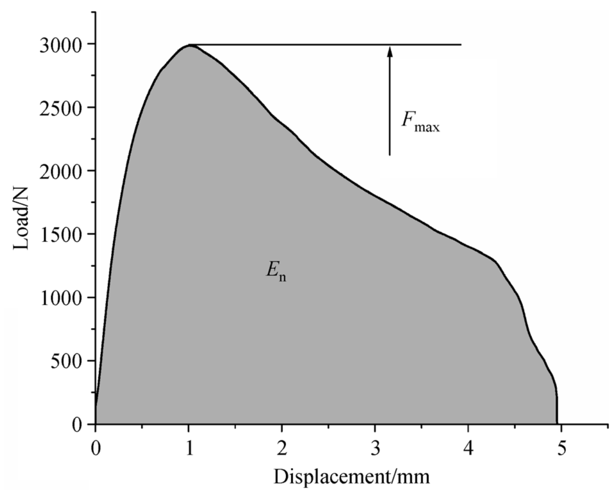

Fig. 5 Schematic diagram of joint energy absorption definition.

4 Results and discussion

4.1 Cross-section profile and characteristic parameters of the clinched joint

The clinched joints with various sheet configurations reported in Fig. 6 showed different cross-sectional profiles. Under the forming load of 90 kN, the mechanical interlock was generated to hook the bottom and top sheets for all clinched samples. A tiny protrusion appeared in the bottom of the 1060 + 2024 sample because the clamping force was slightly insufficient to ensure that the bottom sheet material under the clamp was always in contact with the planar anvil. However, for other clinched samples, the protrusion in the bottom sheet was completely avoided under the clamping force. An annular protrusion appeared in the top sheet for all clinched samples. The 1060 + 2024 sample had a higher annular protrusion than the 2024 + 1060 sample. The 2.5 + 1.5 sample had a slightly lower annular protrusion than the 1.5 + 2.5 sample. The neck portions of the 1060 + 2024 and 1.5 + 2.5 samples were significantly elongated. The material of the bottom sheet was not enough to flow into the interlock area; thus, a gap appeared between the bottom and top sheets. However, the gap did not appear in the 2024 + 1060 and 2.5 + 1.5 samples. These results indicated that material and thickness configurations performed vital roles in the geometric profile of the flat clinched joint.

The characteristic parameters of the clinched joint were determined from the cross-sectional profiles of the clinched samples. The characteristic parameters of the clinched joints with various sheet configurations are depicted in Fig. 7. The 1060 + 2024 joint demonstrated a 7.3% larger U_d and a 73.8% lower N_t than the 2024 + 1060 joint. The 1.5 + 2.5 joint showed 4.58 times higher U_d and 67.1% smaller N_t than the 2.5 + 1.5 joint. Besides, the 2024 + 1060 joint had the biggest N_t, while the 2.5 + 1.5 joint had the lowest U_d.

The Al2024 sheet exhibited higher tensile strength and stiffer property than the Al1060 sheet. As depicted in Fig. 8, the material flow is presented using arrows in the flat clinching process. The material of the sheets under the clamp could not flow under the action of the high clamping force. The neck portion of the top sheet was elongated. A part of the neck material was pressed into the gap between the clamp and the punch. Another part of the neck material flowed into the bulging bottom of the top sheet. For the joint using a stiff bottom sheet, the material of the top sheet was exceedingly difficult to be squeezed into the cavity of the bottom sheet because the bottom sheet was stiffer than the top sheet. A small amount of material in the top sheet was squeezed into the groove of the bottom sheet. Therefore, the U_d and N_t of the joint were small. A large amount of material on the top sheet converged on its circular protrusion to improve the height of the protrusion. For the joint using a stiff top sheet, the material of the top sheet could easily flow into the cavity of the bottom sheet because the top sheet had higher mechanical resistance than the bottom sheet. Several compressed materials in the top sheet flowed to the neck portion, and a small amount of material flowed into the gap. Besides, the material of the bottom sheet was difficult to flow into the interlocking area due to the higher mechanical resistance of the top sheet. Therefore, the joint using the stiff top sheet had smaller

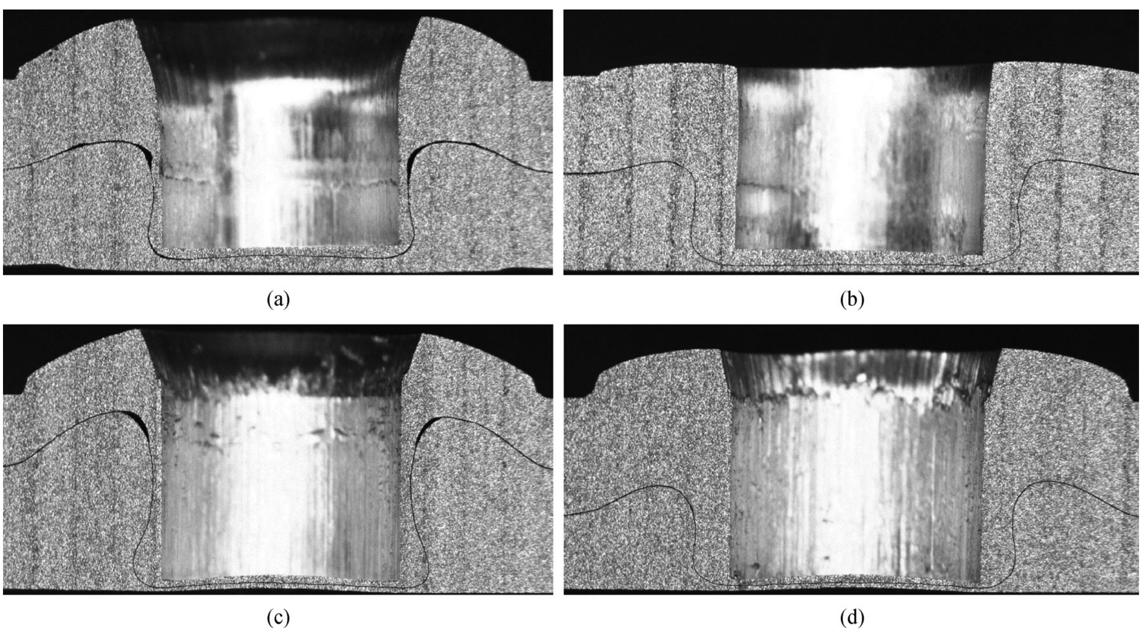

Fig. 6 Cross-sectional profiles of clinched joints with various sheet configurations: (a) 1060 + 2024 joint; (b) 2024 + 1060 joint; (c) 1.5 + 2.5 joint; and (d) 2.5 + 1.5 joint.

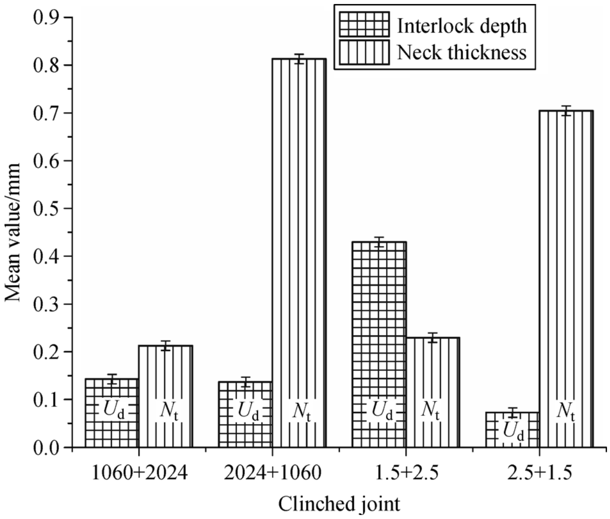

Fig. 7 Characteristic parameters of the clinched joints with various sheet configurations.

protrusion height, higher N_t, and smaller U_d than that using the stiff bottom sheet.

The material flow of the flat clinched samples with different thickness configurations is illustrated in Fig. 9. For the joint using a thick bottom sheet, the neck portion of the top sheet was significantly elongated owing to a high stamping depth and a thin initial thickness of the top sheet. Meanwhile, because the bottom sheet was thicker than the top sheet, more materials on the bottom sheet was compressed into the interlocking area. Given the large amount of bottom sheet material moving upward, the top sheet material was jacked up and flowed into the gap. Thus, the circular protrusion in the top sheet was high. For the joint using a thick top sheet, the punching depth of the top sheet was lower, and the top sheet had more compressed material flowing into the neck portion; thus, the thinning of the neck portion in the top sheet was minimal. Besides, the bottom sheet has less material squeezed into the interlocking area. Therefore, the joint using the thick top sheet had stronger neck portion and weaker interlock than that using the thick bottom sheet.

4.2 Static strength and failure mode

Static strength can be used to access the joint quality. The higher the static strength of the clinched joint, the better the joining quality. The tensile strength is a commonly used type of joint static strength. In this study, it was acquired from the load–displacement curve in the cross-tensile test. The failure modes and typical load–displacement curves for the various clinched samples in the cross-tensile tests are presented in Fig. 10. On the whole, the evolutions of the load–displacement curves showed a similar development trend. The initial load–displacement curves characterizing the stiffness of the joint were close. With the increase in the displacement, the curve load–displacement

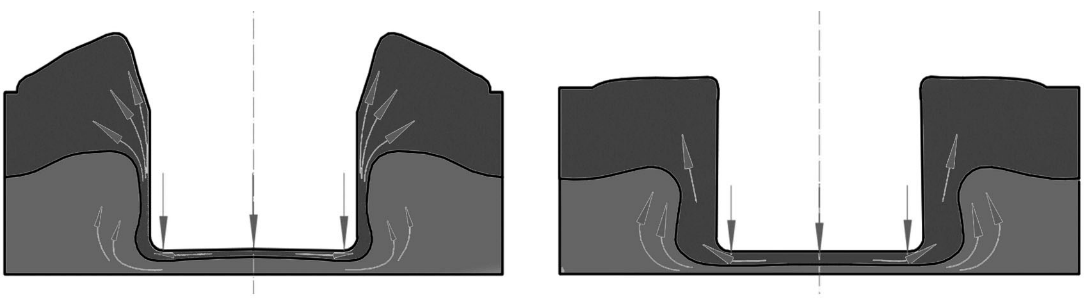

(a) (b)

Fig. 8 Schematic of material flow for the flat clinched sample using different material configurations: Sample using the stiff (a) bottom sheet and (b) top sheet.

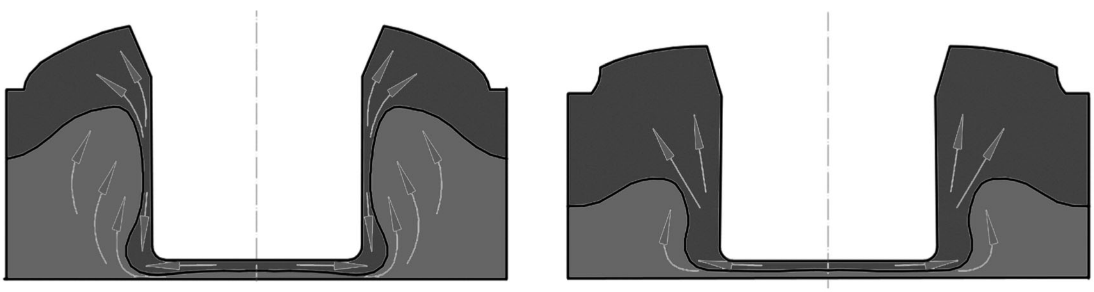

(a) (b)

Fig. 9 Schematic of material flow for the flat clinched samples with different thickness configurations: Sample using thick (a) bottom sheet and (b) top sheet.

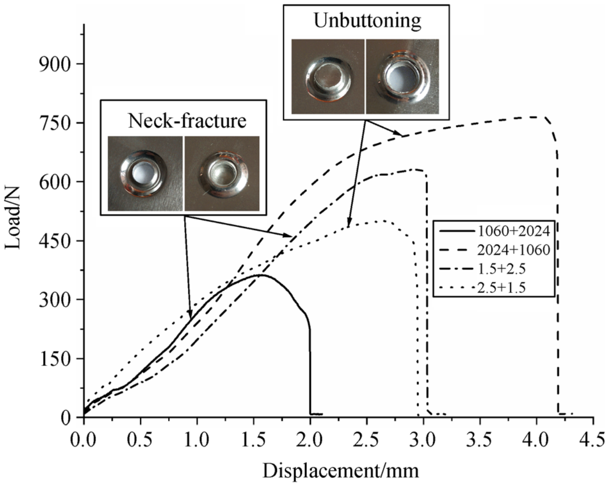

Fig. 10 Failure modes and typical load versus displacement for the clinched samples using different sheet configurations in cross-tensile tests.

gradually increased to maximum load (F_{max}), which was regarded as the strength of the clinched joint. The strength of the joint considerably differed. The curves dropped rapidly after the load peaked. In addition, the 2024 + 1060 sample had longer tensile displacement than the other sample. The joint failed when the tensile load reached the joint strength. The 1060 + 2024 and 1.5 + 2.5 joints failed in the neck-fracture mode, while the 2024 + 1060 and 2.5 + 1.5 joints lost effectiveness in the unbuttoning mode.

Figure 11 shows the tensile strengths of the various clinched joints. The tensile strength of the 2024 + 1060 joint was 769.5 N, the largest of all. The 1060 + 2024 joint demonstrated the smallest tensile strength. The tensile strength of the 1060 + 2024 joint decreased by 52.5% compared with that of the 2024 + 1060 joint. The tensile strength of the 1.5 + 2.5 joint was 640.4 N, 27.4% higher than that of the 2.5 + 1.5 joint. The effect of thickness configuration on the tensile strength of the joint was smaller than that of the material configuration.

Changes in the material and thickness configurations cause changes in failure modes and tensile strength. The load was concentrated in the fragile area of the joint during the cross-tensile test. For the clinched joints using stiff or thick bottom sheet, F_n was further lower than F_u. The tensile load was mainly exerted on the neck portion of the clinched joint. When the tensile load reached F_n, the clinched joint failed. Therefore, the 1060 + 2024 and 1.5 + 2.5 joints failed in the neck-fracture mode. For the clinched joints with stiff or thick top sheets, $F_u \ll F_n$. The tensile load was mainly applied to the interlock area of the clinched joint. Once the tensile load reached F_u, the clinched joint failed. Therefore, the 2024 + 1060 and 2.5 + 1.5 joints lost effectiveness in the unbuttoning mode. As the F_n of the 1060 + 2024 joint was lower than F_u of the 2024 + 1060 joint, the tensile strength of the 1060 + 2024 joint was smaller than that of the 2024 + 1060 joint. The 1.5 + 2.5 joint had larger tensile strength than the 2.5 + 1.5 joint because the F_n of the 1.5 + 2.5 joint was higher than F_u of the 2.5 + 1.5 joint. These results indicated that the clinched joint with stiff top sheet had larger tensile strength than the clinched joint using stiff bottom sheet. The tensile strength of the clinched joint with thick top sheet was lower than that of the clinched joint using thick bottom sheet.

Shearing strength is another commonly used type of joint static strength. In this study, it was acquired from the load–displacement curve in the shearing test. Figure 12 shows the failure modes and typical load–displacement curves for the various clinched samples in the shearing tests. The failure modes and load–displacement curves of the 2024 + 1060 and 2.5 + 1.5 samples exhibited the same development trend, while the load–displacement curves of

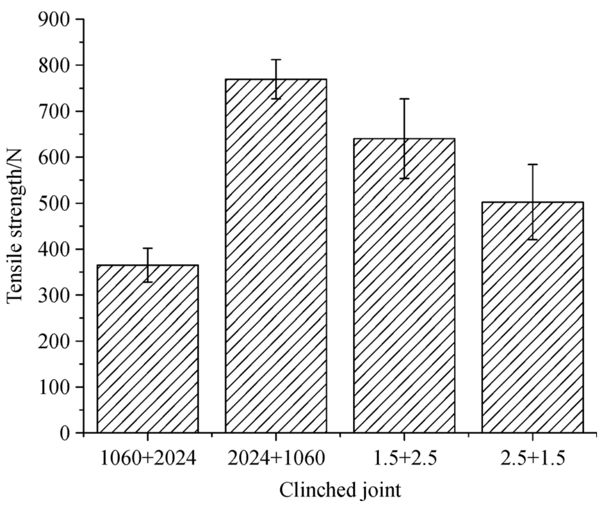

Fig. 11 Tensile strengths of the clinched joints using various sheet configurations.

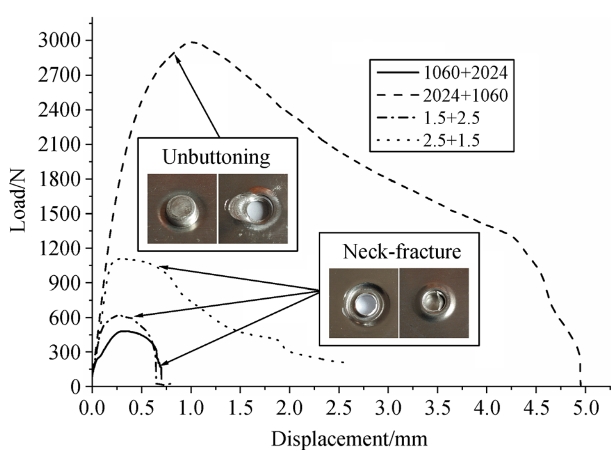

Fig. 12 Failure modes and typical load–displacement curves for the clinched samples using different sheet configurations in shearing tests.

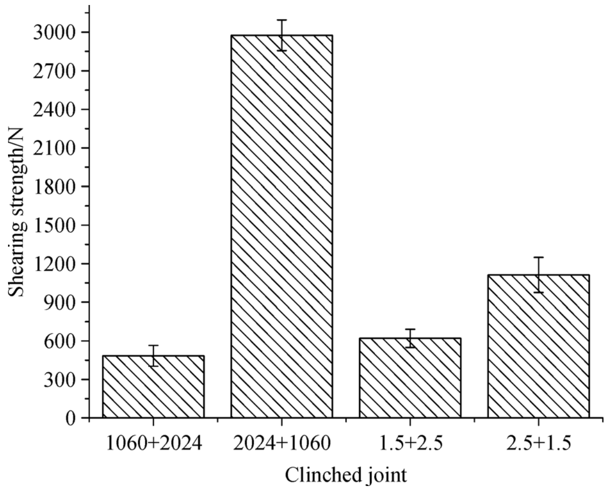

Fig. 13 Shearing strengths of various clinched joints.

the 1060 + 2024 and 1.5 + 2.5 samples demonstrated the same development trend. Initially, the load–displacement curves were coincidental. The shearing load quickly increased to the maximum load with the increase in displacement. The maximum loads exhibited an obvious difference. For the 1060 + 2024 and 1.5 + 2.5 samples, the load–displacement curves dropped steeply. For the 2024 + 1060 and 2.5 + 1.5 samples, the loads decreased slowly. The 2024 + 1060 sample had longer shearing displacement than the other samples. When the shearing loads reached the maximum loads, the 2024 + 1060 joint failed in the unbutton-failure mode, and the other joints lost effectiveness in neck-fracture mode.

The shearing strengths of the various clinched joints are reported in Fig. 13. The 2024 + 1060 joint showed an obviously larger shearing strength than the other clinched joints. The shearing strength of the 1060 + 2024 joint was 485.3 N, the smallest of all. It was 0.16 times that of the 2024 + 1060 joint. The 1.5 + 2.5 joint had a shearing strength of 618.7 N. The shearing strength of the 2.5 + 1.5 joint increased by 79.8% than that of the 1.5 + 2.5 joint.

The Al2024 sheet showed a significantly higher mechanical resistance than the 1060 sheet. Besides, the 2024 + 1060 joint had the biggest N_t in this study. The bulge of the top sheet was difficult to deform plastically. Therefore, the 2024 + 1060 sample had a significantly higher shearing strength than the other clinched joints. The interlock failure of the 2024 + 1060 joint during the shearing test was extremely formidable. After the joint failed, its top sheet bulge continuously pushed the material of the bottom sheet to make it flow plastically and plowed out a groove, which is called the furrow effect. The sample had a longer shearing displacement because of the furrow effect. For the other clinched joints, the neck portion of the top sheet underwent most of the shearing force. The shearing strength of the joints depended on the material and N_t of the top sheet. The 2.5 + 1.5 joint had a larger N_t than the 1.5 + 2.5 and 1060 + 2024 joints. Thus, the shearing strength of the 2.5 + 1.5 joint was higher than that of the other two samples. The N_t of the 1060 + 2024 joint was the lowest. Therefore, the 1060 + 2024 joint had the lowest shearing strength. These results indicated that the shearing strength of the clinched joint with stiff top sheet was higher than that of the clinched joint with stiff bottom sheet. The clinched joint with thick top sheet had a larger shearing strength than that with thick bottom sheet.

The absorbed energy of the different clinched samples in the cross-tensile and shearing tests is shown in Fig. 14. Regardless of the test type, the energy absorption trend was most consistent with the static strength trend. The 2024 + 1060 joint had a longer displacement than the other samples in the shearing test because of the furrow effect. Meanwhile, the 2024 + 1060 joint had the largest shearing strength. Therefore, its absorbed energy was significantly higher. The 2024 + 1060 joint had 3.67 times higher energy absorption than the 1060 + 2024 joint in the cross-tensile test. The energy absorption of the 1.5 + 2.5 joint is slightly larger than that of the 2.5 + 1.5 joint in the cross-tensile test, while the 2.5 + 1.5 joint had higher absorbed energy than the 1.5 + 2.5 joint in the shearing test.

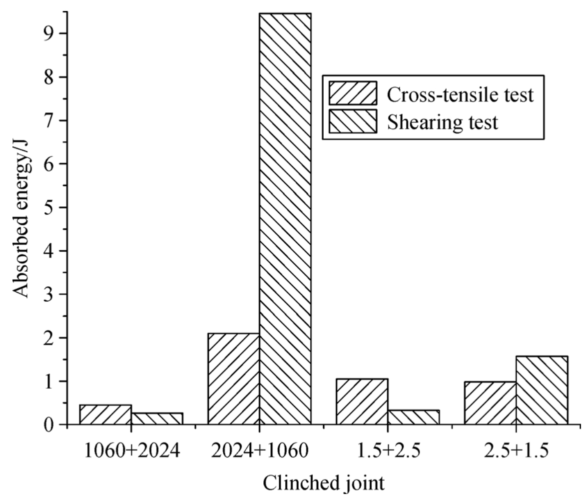

Fig. 14 Absorbed energy of the clinched samples using various sheet configurations in cross-tensile and shearing tests.

5 Conclusions

In this paper, the effect of sheet thickness and material on the mechanical properties of the flat clinched joint was systematically studied. The 1060 sheets and 2024 sheets with 2 mm thickness were employed to produce the clinched samples with different material configurations. The 1060 sheets with 1.5- and 2.5-mm thickness were utilized for developing the clinched samples with different thickness configurations. Under the forming force of 90 kN, the clinched samples were joined by mechanical interlock. The material flow was analyzed to understand the differences in specimen geometry. The static strength, failure mode, and absorbed energy was studied and discussed in detail to present the mechanical properties of the flat clinched joint. The following conclusions can be summarized:

1) The clinched joint with a stiff top sheet has larger N_t and smaller U_d than the clinched joint with a stiff bottom sheet due to the higher mechanical resistance of the top sheet.

2) The clinched joint with a thick bottom sheet has larger U_d and smaller N_t than that with a thick top sheet because of the high stamping depth, the thin initial thickness of the top sheet, and a large amount of the bottom sheet material moving upward.

3) Regardless of the test type, the clinched joint using a stiff bottom sheet has lower static strength and absorbed energy than the joint with a stiff top sheet.

4) In the cross-tensile test, the clinched joint with a thick top sheet has lower static strength and absorbed energy than that with a thick bottom sheet because the tensile structural strength of itsinterlock was lower than the neck portion of the joint with a thick bottom sheet.

5) In the shearing test, the clinched joint with a thick top sheet has higher static strength and absorbed energy because of larger N_t.

Acknowledgements This research work was supported by the National Natural Science Foundation of China (Grant No. 51805416), the Young Elite Scientists Sponsorship Program by CAST, the Natural Science Foundation of Hunan Province, China (Grant No. 2020JJ5716), the Natural Science Basic Research Plan in Shaanxi Province of China (Grant No. 2019JQ-372), the Research Fund of State Key Laboratory of High Performance Complex Manufacturing (Grant No. ZZYJKT2019-01), and the Huxiang High-Level Talent Gathering Project of Hunan Province, China (Grant No. 2019RS1002).

References

1. Lambiase F. Influence of process parameters in mechanical clinching with extensible dies. International Journal of Advanced Manufacturing Technology, 2013, 66(9–12): 2123–2131
2. Song Y, Yang L, Zhu G, et al. Numerical and experimental study on failure behavior of steel–aluminium mechanical clinched joints under multiple test conditions. International Journal of Lightweight Materials and Manufacture, 2019, 2(1): 72–79
3. Lei L, He X, Yu T, et al. Failure modes of mechanical clinching in metal sheet materials. Thin-Walled Structures, 2019, 144: 106281
4. Chu M, He X, Zhang J, et al. Clinching of similar and dissimilar sheet materials of galvanized steel, aluminium alloy and titanium alloy. Materials Transactions, 2018, 59(4): 694–697
5. Lee C J, Kim J Y, Lee S K, et al. Parametric study on mechanical clinching process for joining aluminum alloy and high-strength steel sheets. Journal of Mechanical Science and Technology, 2010, 24(1): 123–126
6. Tenorio M B, Lajarin S F, Gipiela M L, et al. The influence of tool geometry and process parameters on joined sheets by clinching. Journal of the Brazilian Society of Mechanical Sciences and Engineering, 2019, 41(2): 67
7. Lambiase F, Di Ilio A. An experimental study on clinched joints realized with different dies. Thin-Walled Structures, 2014, 85: 71–80
8. Abe Y, Kato T, Mori K I, et al. Mechanical clinching of ultra-high strength steel sheets and strength of joints. Journal of Materials Processing Technology, 2014, 214(10): 2112–2118
9. Mucha J, Kaščák L, Spišák E. Joining the car-body sheets using clinching process with various thickness and mechanical property arrangements. Archives of Civil and Mechanical Engineering, 2011, 11(1): 135–148
10. Abe Y, Saito T, Mori K I, et al. Mechanical clinching with dies for control of metal flow of ultra-high-strength steel and high-strength steel sheets. Proceedings of the Institution of Mechanical Engineers, Part B: Journal of Engineering Manufacture, 2018, 232(4): 644–649
11. Varis J P. The suitability of round clinching tools for high strength structural steel. Thin-Walled Structures, 2002, 40(3): 225–238
12. Lambiase F. Mechanical behaviour of polymer–metal hybrid joints produced by clinching using different tools. Materials & Design, 2015, 87: 606–618
13. Lambiase F, Di Ilio A. Optimization of the clinching tools by means of integrated FE modeling and artificial intelligence techniques. Procedia CIRP, 2013, 12: 163–168
14. Hamel V, Roelandt J, Gacel J, et al. Finite element modeling of clinch forming with automatic remeshing. Computers & Structures, 2000, 77(2): 185–200
15. Lambiase F. Joinability of different thermoplastic polymers with aluminium AA6082 sheets by mechanical clinching. International Journal of Advanced Manufacturing Technology, 2015, 80(9–12): 1995–2006
16. Abe Y, Mori K, Kato T. Joining of high strength steel and aluminium alloy sheets by mechanical clinching with dies for control of metal flow. Journal of Materials Processing Technology, 2012, 212(4): 884–889
17. Neugebauer R, Kraus C, Dietrich S. Advances in mechanical joining of magnesium. CIRP Annals, 2008, 57(1): 283–286
18. Kaðèák L, Spiðák E, Kubík R, et al. Finite element calculation of clinching with rigid die of three steel sheets. Strength of Materials, 2017, 49(4): 488–499
19. Kaščák L, Mucha J, Spisak E, et al. Wear study of mechanical clinching dies during joining of advanced high-strength steel sheets. Strength of Materials, 2017, 49(5): 726–737
20. Sabra Atia M K, Jain M K. A parametric study of FE modeling of die-less clinching of AA7075 aluminum sheets. Thin-Walled Structures, 2018, 132: 717–728
21. Atia M K S, Jain M K. Finite element analysis of material flow in die-less clinching process and joint strength assessment. Thin-Walled Structures, 2018, 127: 500–515
22. Gerstmann T, Awiszus B. Recent developments in flat-clinching. Computational Materials Science, 2014, 81: 39–44
23. Lüder S, Härtel S, Binotsch C, et al. Influence of the moisture content on flat-clinch connection of wood materials and aluminium. Journal of Materials Processing Technology, 2014, 214(10): 2069–2074

24. Han X, Zhao S, Chen C, et al. Optimization of geometrical design of clinching tools in flat-clinching. Journal of Mechanical Engineering Science, 2017, 231(21): 4012–4021
25. Chen C, Zhao S, Han X, et al. Experimental investigation on the joining of aluminum alloy sheets using improved clinching process. Materials, 2017, 10(8): 887
26. Chen C, Zhao S, Han X, et al. Investigation of flat clinching process combined with material forming technology for aluminum alloy. Materials, 2017, 10(12): 1433
27. Varis J P. The suitability of clinching as a joining method for high-strength structural steel. Journal of Materials Processing Technology, 2003, 132(1–3): 242–249
28. Chen C, Zhao S, Han X, et al. Experimental investigation of the mechanical reshaping process for joining aluminum alloy sheets with different thicknesses. Journal of Manufacturing Processes, 2017, 26: 105–112
29. Chen C, Han X, Zhao S, et al. Influence of sheet thickness on mechanical clinch–compress joining technology. Journal of Process Mechanical Engineering, 2018, 232(6): 662–673
30. He X, Zhang Y, Xing B, et al. Mechanical properties of extensible die clinched joints in titanium sheet materials. Materials & Design, 2015, 71: 26–35
31. Chen C, Han X, Zhao S, et al. Comparative study on two compressing methods of clinched joints with dissimilar aluminum alloy sheets. International Journal of Advanced Manufacturing Technology, 2017, 93(5–8): 1929–1937
32. Eshtayeh M M, Hrairi M. Recent and future development of the application of finite element analysis in clinching process. International Journal of Advanced Manufacturing Technology, 2016, 84(9–12): 2589–2608
33. de Paula A A, Aguilar M T P, Pertence A E M, et al. Finite element simulations of the clinch joining of metallic sheets. Journal of Materials Processing Technology, 2007, 182(1–3): 352–357
34. Mucha J. The analysis of lock forming mechanism in the clinching joint. Materials & Design, 2011, 32(10): 4943–4954
35. Pietrapertosa C, Zhang L, Habraken A, et al. Clinching joining system: Validation of numerical models. In: Proceedings of the 6th International ESAFORM Conference on Material Forming. Salerno: Nuova Ipsa editire, 2003, 351–354
36. Xu F, Zhao S, Han X. Use of a modified Gurson model for the failure behaviour of the clinched joint on Al6061 sheet. Structures Fracture of Engineering Materials, 2014, 37(3): 335–348
37. Zhao S, Xu F, Guo J, et al. Experimental and numerical research for the failure behavior of the clinched joint using modified Rousselier model. Journal of Materials Processing Technology, 2014, 214(10): 2134–2145
38. He X, Zhao L, Yang H, et al. Investigations of strength and energy absorption of clinched joints. Computational Materials Science, 2014, 94: 58–65
39. Lei L, He X, Zhao D, et al. Clinch-bonded hybrid joining for similar and dissimilar copper alloy, aluminium alloy and galvanised steel sheets. Thin-Walled Structures, 2018, 131: 393–403